ISME

Iranian Journal of Mechanical Engineering
The Iranian Society of Mechanical Engineers
Research Paper

DOI: 10.30506/jmee.2020.121751.1226

Enhancement of Sound Absorber by Multi-area Helmholtz Resonators Array Based on Fibonacci Sequence

S. Saffar*
Associate Professor

This paper try to show that cling to the physical order that governs nature can be helpful in engineering application such as acoustical materials. In this regards, an innovative idea to the noise control problem for broader absorption bandwidth at low frequencies is presented in this paper. For this aim, Helmholtz resonator array (HRA) designed based on Fibonacci sequence, which is addressed "Fibonacci based-HRA". First, to validate the simulations which were performed through finite element method (FEM) as a numerical method in COMSOL Multi-physics software (Version 5.2), the results have been compared with experimental results which obtained by other researchers for two cases: (1) one unit resonator, and (2) four resonators array block with equal size. Second, to examine the performance of sound absorption of Fibonacci based-HRA, the results obtained for HRA with equal sizes of the 4, 6, 8 and 10 component resonators, compared with those obtained for Fibonacci based-HRA with the same number of the component resonators and the same overall dimensions of HRA block. The comparison showed that Fibonacci based-HRA approach is a good candidate for broad-band low frequency noise control.

Keywords: Fibonacci based Helmholtz resonator array (Fibonacci based-HRA), sound absorption coefficient, broad-band low frequency noise control, finite element method (FEM)

1 Introduction

At the time being, the sound pollution especially in metropolises, is a critical issue. Therefore, there exist an increasing trend toward the usage and the design of more effective sound absorbers. The conventional sound absorbing materials like porous materials (fibers and foams) are well suited for mid and high frequency noise control [1-3]. Some researchers have been shown that using air gap can be helpful to increase the sound absorption in low frequency [4]. Although, increasing the thickness of the porous absorber causes more absorber causes more absorption at low frequency it is not applicable because of large dimension of absorber elements.in fact, space limitation always is a critical issue in acoustical design. By increasing the thickness of the porous media, more absorption performance occurs at low frequency bands too. In (2017), Kim and his colleague proposed double resonant porous structure backed by air cavity for low frequency sound absorption [4]. Up to now, many researchers proposed different resonant sound absorbers such as micro-perforated panel

* Corresponding Author, Associate Professor, Department of Acoustics and Sound Engineering, IRIB University, P.O. Box 1986916511, Tehran, Iran saffar@IRIBU.ac.ir
Receive : 2020/02/16 Accepted : 2020/10/04

(MPP) [5] and Helmholtz resonator (HR) [6] to improve the sound absorption at the low frequency band and to reduce the total thickness. Another approaches to broaden the sound absorption bandwidth are parallel arrangement of multiple MPP [7-9], MPP backed by uniform air gap [10-12], MPP backed by partitioned cavity [13-15], MPP backed by incompletely partitioned cavities [16], MPP with tube bundles [17-19], MPP backed by different cavity depth [20-23] and HR array panel [24, 25]. Maximum sound absorption coefficient of a resonant absorber occurs in it is resonance frequency and rapidly decreases beyond its resonance frequency, in other word, resonant absorbers work very well in narrow band frequency which is not enough in acoustical design point of view. In this regards, Seo and his colleague [26] proposed a resonator array panel absorber consists of some number of the same Helmholtz resonators where located near each other periodically for low frequency band noise reduction. Based on previous discuss, Helmholtz resonator array (HRA) is still unsuitable for broad-band low frequency sound absorption. It is necessary to increase the number of frequency resonances due to increase the number of resonator with different geometrical dimensions. Hence, it seems that broader absorption bandwidth in low frequency can be achieved be using of multi size Helmholtz resonators. Fibonacci can be found in nature not only in the famous rabbit experiment, but also in beautiful flowers [27]. On the head of a sunflower and the seeds are packed in a certain way so that they follow the pattern of the Fibonacci sequence. This spiral prevents the seed of the sunflower from crowding themselves out, thus helping them with survival. The petals of flowers and other plants may also be related to the Fibonacci sequence in the way that they create new petals [28]. Fibonacci spiral [29, 30] is also found in various fields associated in nature. It is seen snail, sea shells, waves, combination of colors; roses etc in so many things created in nature [27]. But very few of us have time to study this phenomenon. Some samples of Fibonacci sequence are shown in Fig. (1). Nature isn't trying to use the Fibonacci numbers: they are appearing as a by-product of a deeper physical process. That is why the spirals are imperfect. The plant is responding to physical constraints, not to a mathematical rule. The basic idea is that the position of each new growth is about 222.5 degrees away from the previous one, because it provides, on average, the maximum space for all the shoots. This angle is called the golden angle, and it divides the complete 360 degree circle in the golden section, 0.618033989 . . . . which is described below. Organs of human body Humans exhibit Fibonacci characteristics.

Every human has two hands, each one of these has five fingers and each finger has three parts which are separated by two knuckles [31]. All of these numbers fit into the sequence. Moreover the lengths of bones in a hand are in Fibonacci numbers.

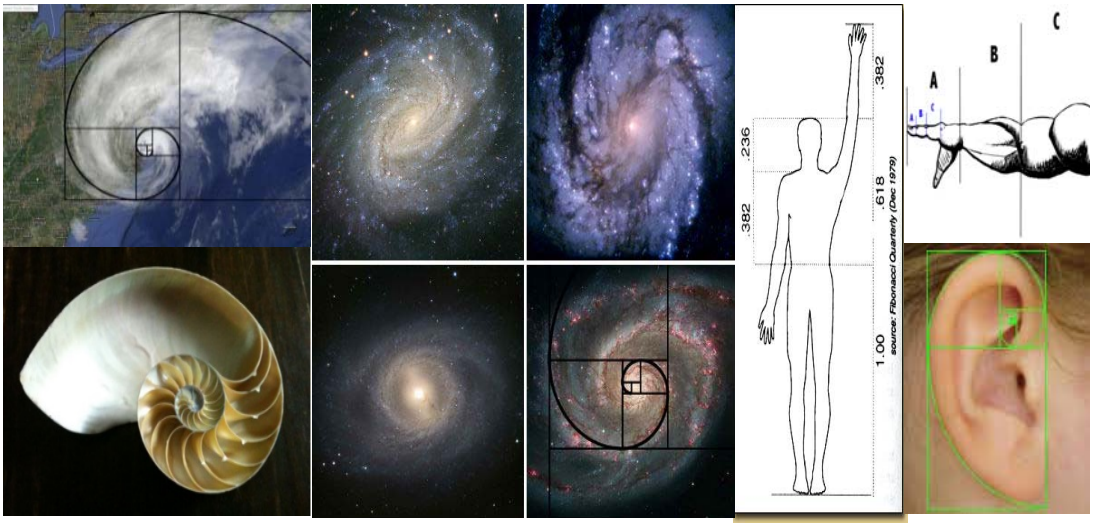

Figure 1 Samples of the Fibonacci golden spiral and the golden ratio based on Fibonacci sequence in nature

Therefore, Fibonacci sequence is famous mathematical model which is found in the nature easily. In addition, the physical fact which mentions that every physical phenomenon tends to minimize their energy in absence of external forces is driving force of the author that maybe Fibonacci sequence to be a consequence of the minimizing energy in the physical phenomenon in the world. Therefore, author has been believed that Fibonacci sequence, could be good candidate to design a multi size HRA with minimum size but maximum sound absorption in broaden frequency band in low frequencies. In this regards, author proposed a new arrangement for Helmholtz component resonators in a sound absorber block, in which the length of each side of the Helmholtz component resonators and their hole diameters vary based on the Fibonacci sequence. To the authors' investigation and evaluation, there is no report about way of arrangement of Helmholtz resonators where locate as array next to each other based on Fibonacci sequence to increase the sound absorption coefficient and frequency bandwidth of sound absorption, especially at low frequencies.

2 Theory

2.1 Theory of Fibonacci sequence

The Fibonacci numbers were first discovered by a man named Leonardo Pisano. He was known by his nickname, Fibonacci. The Fibonacci sequence is a sequence in which each term is the sum of the 2 numbers preceding it. The Fibonacci Numbers are defined by the recursive relation defined by the equations $F_n = F_{n-1} + F_{n-2}$ for all $n \geq 3$ where $F_1 = 1$; $F_2 = 1$ where F_n represents the n^{th} Fibonacci number (n is called an index).
Classical Fibonacci numbers have been generalized in different ways [32-36]. One of these generalizations that greater interest lately among mathematical researchers is that leads to the k–Fibonacci numbers [37, 38]. Then the k–Fibonacci numbers are defined.

For every natural number k, the k–Fibonacci sequence $F_k = \{F_{k,n}\}$ is defined by the recurrence relation $F_{k,n+1} = k F_{k,n} + F_{k,n-1}$ for $n \geq 1$ with initial conditions $F_{k,0} = 0$; $F_{k,1} = 1$

From this definition, the general expression of the first k–Fibonacci numbers is presented in the following:

$F_{k,0} = 0$
$F_{k,1} = 1$
$F_{k,2} = k$
$F_{k,3} = k^2 + 1$
$F_{k,4} = k^3 + 2k$
$F_{k,5} = k^4 + 3k^2 + 1$
$F_{k,6} = k^5 + 4k^3 + 3k$
$F_{k,7} = k^6 + 5k^4 + 6k^2 + 1$
$F_{k,8} = k^7 + 6k^5 + 10k^3 + 4k \cdots$

If $k = 1$ the classical Fibonacci sequence is obtained $F_1 = \{0, 1, 1, 2, 3, 5, 8, \ldots\}$ and if $k = 2$ that is the Pell sequence $F_2 = P = \{0, 1, 2, 5, 12, 29, 70, 169, \ldots\}$.

3.1 Plane sound waves at normal incidence

For plane waves of sound incident perpendicularly to an absorber it is sufficient to know the complex normal specific surface impedance $Z_1 = Z_1' - jZ_1''$ of the absorber, which is the ratio of sound pressure to the normal component of the particle velocity at the interface.
The reflection factor and absorption coefficient are related by

$$R = \frac{Z_1 - Z_0}{Z_1 + Z_0} \quad \alpha = \frac{4Z_1' Z_0}{(Z_1' + Z_0)^2 + Z_1''^2} \tag{1}$$

Where $Z_0 = \rho_0 c_0$ is the characteristic impedance of air for plane wave, and ρ_0 is the density and c_0 the speed of sound in air [39]. For sound absorbers consisting of highly porous layers with perforated or cloth facings of smaller porosity, a modified air-side surface impedance must be used in Eq.1. This is obtained by tacking the air-side volume velocity averaged over the face area of the absorber. If an absorber with surface impedance Z_R is covered by a perforated facing with porosity ε, then $Z_1 = Z_R/\varepsilon$

4.1 Acoustic impedance of a resonator

The specific acoustical impedance of the resonator opening Z_R is the summation of impedance of the enclosed air volume Z_v and that of the air volume that air volume that oscillates in and around the resonator month Z_m, namely,

$$Z_R = Z_v + Z_m = (z_v' + jz_v'') + (z_m' + jz_m'') \quad [\mathrm{N.s/m^3}] \tag{2}$$

The volume impedance $Z_v = jZ_v^{"}$ is purely imaginary and predominantly of spring character while the mouth impedance has a real part z_m' and an imaginary part z_m'' and is predominantly of mass character. Therefore, the impedance of a rectangular resonator volume can be written as follows:

$$Z_v = -jZ_v^{"} = -j\rho_0 C_0 \, cot(K_0 t)\frac{S_a}{S_b} \quad [\mathrm{N.s/m^3}] \tag{3}$$

Where, as shown in Fig. (2), S_b is the surface area of the resonator cover plate, $S_a = \pi a^2$ is the area of the resonator mouth, t is the depth of the resonator cavity, and $V=S_b\ t$ is the volume of the resonator. Note that if the resonator dimensions are small compared with the wavelength($K_0 t \ll 1$), Eq.3 yields

$$Z_v = jZ_v^{"} = -j\frac{\rho_0 {C_0}^2}{\omega}\frac{S_a}{V} \quad [\mathrm{N.s/m^3}] \tag{4}$$

If the all dimensions are smaller than the wavelength of interest, the shape of cavity has no effect on its application. The acoustic impedance of the resonator mouth Z_m consists of components correspond to the vibration of air internal to the mouth, within the mouth, and external to the mouth of the resonator plus the acoustic impedance of the screen (Z_s) that maybe placed across the resonator mouth to provide resistance. The total acoustic impedance of circular resonator opening of radius a and orifice plate thickness, l, can be written as follows:

$$Z_m' = \rho_0\left[\sqrt{8\vartheta\omega}\left(1+\frac{l}{2a}\right)+\frac{(2\omega a)^2}{16c_0}\right] + z_s \quad [\mathrm{N.s/m^3}] \tag{5}$$

$$Z_m'' = \omega\rho_0\left[l+\left(\frac{8}{3\pi}\right)2a\right]+\left(l+\frac{1}{2a}\right)\sqrt{8\vartheta\omega} \quad [\mathrm{N.s/m^3}] \tag{6}$$

Where ϑ is the kinematic viscosity ($\vartheta = 1.5\times10^{-6}$ $[\mathrm{m^2/s}]$ for air at room temperature). The quantity $0.5\ (\frac{8\vartheta}{\omega})^{1/2}$ is the viscous boundary layer thickness [39].
Generally, the first term of Eq. 5 depend on surface roughness and it only applied for smooth orifice edges. The value of this can be increased too much for sharp orifice edges.

Also, the second term of Eq. 6 is usually small compared with the first term and can be neglected.

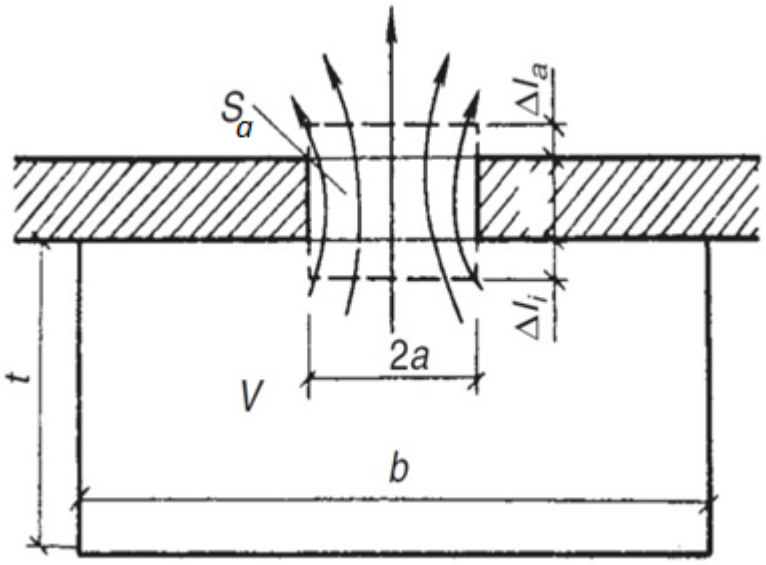

Figure 2 Helmholtz resonator geometry definition [39]

Consequently, Eqs, 5 and 6 for circular orifices and for a single resonator can be generalized for other orifice shapes and for situations where the orifice is located on a large wall or at a two-or three-dimensional corner. This generalized form is:

$$Z'_m = \frac{P(l+p/2\pi)}{4S_a}\rho_0\sqrt{8\vartheta\omega} + \rho_0 c_0 \frac{k_0^2 S_a/\Omega}{1+k_0^2 S_a/\Omega} + z_s \quad [\mathrm{N.s/m^3}] \tag{7}$$

$$Z''_m = j\omega\rho_0\left[l + 2\Delta l + \frac{P(l+p/2\pi)}{4S_a}\sqrt{8\vartheta/\omega}\right] \quad [\mathrm{N.s/m^3}] \tag{8}$$

Where P, S_a and Ω are the perimeter of the orifice, its surface area, and the spatial angle the resonator " looks into", respectively :

$$\Omega = \begin{cases} 4\pi & \text{for resonator away from all wall} \\ 2\pi & \text{flush mounted on wall far from corners} \\ 2\pi & \text{flush mounted on wall at two } - \text{dimensional corners} \\ {}^1/_2\,\pi & \text{flush mounted on wall at three } - \text{dimensional corners} \end{cases} \tag{9}$$

Also, the quantity $\Delta l = 16a/3\pi$ employed for the combined internal and external end corrections [39].

5.1 Resonance frequency

The resonance frequency f_0 of the Helmholtz resonator occurs when Z''_m and Z''_v to be equal in magnitude. It means that Eqs. 4 and 6 should be combined and after mathematical work, resonance frequency can be written as follow:

$$f_0 = \frac{c_0}{2\pi}\sqrt{\frac{s_a}{V\{\ldots\}}} \cong \frac{c_0}{2\pi}\sqrt{\frac{s_a}{V(l+16a/3\pi)}} \tag{10}$$

Where $\{\ldots\} = l + \Delta l$ represents the quantity in square brackets in Eq.8. Also, the viscos term correspond to the Eq. 6 ignored in Eq. 10 because the viscous contribution is small [39].

6.1 Absorption cross section of individual resonators

For a single resonator (or some number of resonators that distances between them are long enough to neglect of the interaction between resonators) cross section of area absorption, *A*, must be considered instead of absorption coefficient α.
The absorption cross section *A* is defined as that surface area (perpendicular to the direction of sound incidence) through which, in the undistributed sound wave (resonator not present), the same sound power would flow through as the sound power absorbed by the resonator.

The sound power which is dissipated in the resonator mouth is:

$$W_m = 0.5|\vartheta|^2 S_a R_T = \frac{0.5\times 2^n |p_{inc}|^2 S_a R_T}{|Z_R|^2} [\mathrm{W}] \tag{11}$$

Accordingly, the absorption by cross section can be calculated by:

$$A = \frac{2^n \rho_0 c_0 S_a R_T}{|Z_R|^2} \quad [\mathrm{m}^2] \tag{12}$$

Where *n=0* for resonators placed in free filed, *n=1* if the resonators are flush mounted in a wall, *n=2* if the resonators are at the junction of two planes, and finally, *n=3* if the resonators are in a corner; $R_T = Z'_m + Z_{rad}$ is the total resistance[39].

A_t the resonance frequency f_0, where $Z''_v + Z''_m = 0$, the absorption cross section reaches its maximum value A_0 :

$$A = 2^n \frac{S_a \rho_0 c_0}{R_{rad}} \left[\frac{R_T/R_{rad}}{|1+R_T/R_{rad}|^2}\right] \quad [\mathrm{m}^2] \tag{13}$$

For a flush-mounted (*n=1*) circular resonator area $S_a = \pi a^2$, the radiation resistance is $R_{rad} = 2(\pi a)^2 \rho_0 c_0 / \lambda_0^2$, and Eq.12 yields

$$A = \frac{1}{\pi}\lambda_0^2 \left[\frac{R_T/R_{rad}}{|1+R_T/R_{rad}|^2}\right] \quad [\mathrm{m}^2] \tag{14}$$

Where λ_0 is the wavelength at the resonance frequency of the resonator. The maximum value of the absorption cross section is obtained by matching the interval resistance to the radiation resistance at the resonance frequency, yielding ($R_T = R_{rad}$)

$$A_0^{max} = \frac{1}{4\pi}\lambda_0^2 \quad [\mathrm{m}^2] \tag{15}$$

3 modeling

In this paper, as it is shown in Fig. (3), area of Helmholtz resonator based on Fibonacci sequence is proposed as shown in Fig. (3), the size of each cell and corresponding hole diameter, calculated based on Fibonacci sequence. For example, 8 cavities with different sizes (different dimension of length and width and different hole diameter) have illustrated in Fig. (3). Every cavity has its own resonance frequency, obviously. Furthermore, it is possible to find many algorithms to arrange many different resonant cavities which seat to each other. One algorithm can be based on the Fibonacci sequence due to the previous explanations.

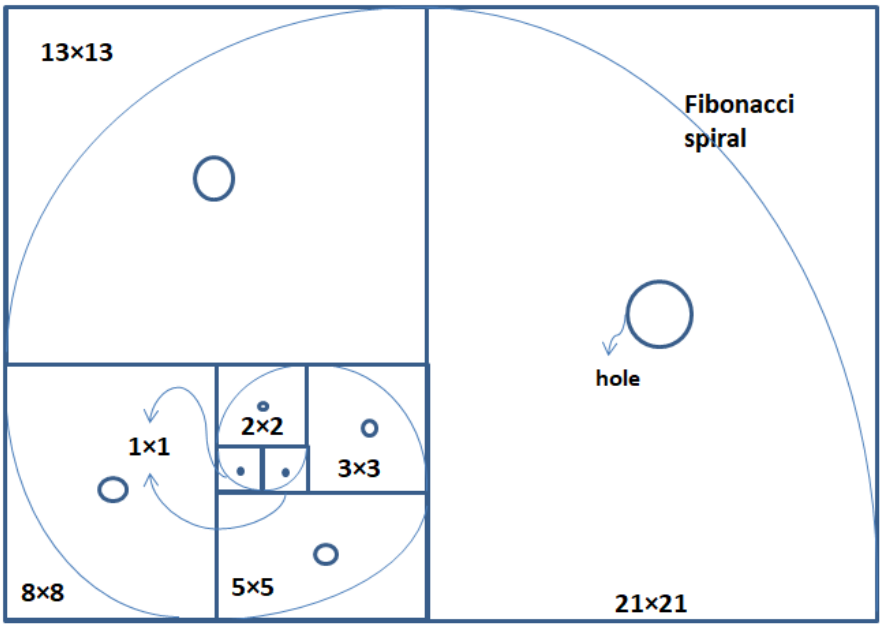

Figure 3 Schematic of Helmholtz resonator area based on Fibonacci sequence

In this paper, many simulations have been carried out using finite element method (FEM) as a numerical method in COMSOL Multi-physics software (Version 5.2). Therefore, to validate, the results have been compared with those experimentally obtained by other researchers for two cases: (1) one unit resonator, and (2) four resonators array block with equal size. Afterwards, the results obtained for HRA composed of 4, 6, 8 and 10 component resonators with equal size, were compared with those obtained by Fibonacci based-HRA with the same number of component resonators and the same overall dimensions of HRA block. The comparison showed that Fibonacci based-HRA is a good candidate for noise control in low frequency range. In previous studies, periodic array of Helmholtz resonator elements with different cross section shapes (as it is shown in Fig. 4) is used to configure sound absorbers for noise control [40].

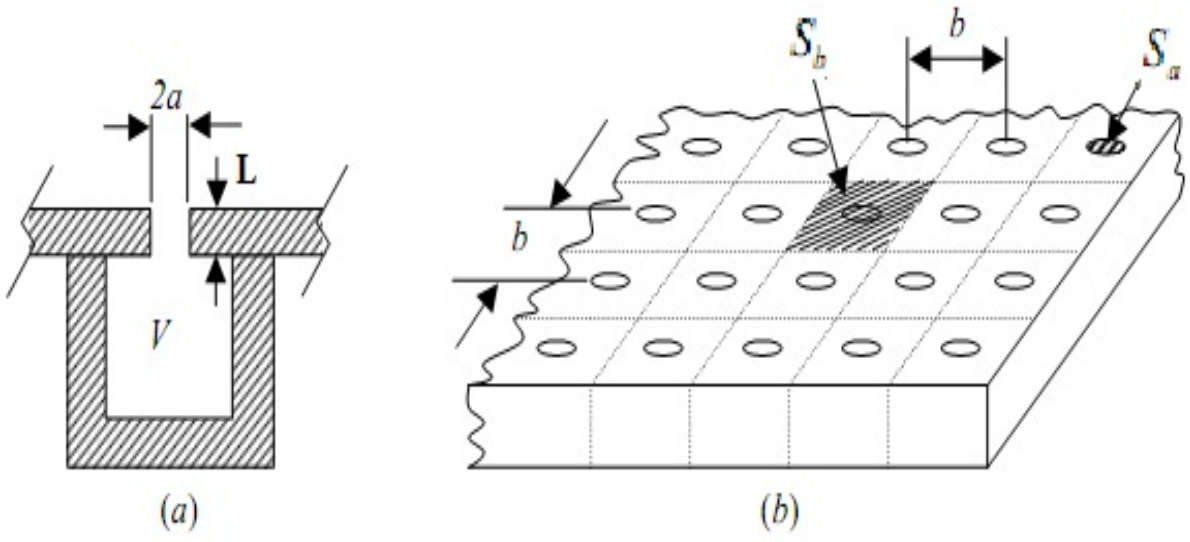

Figure 4 Configuration of Helmholtz resonator array, **(a)** cross section of a resonator unit, **(b)** view of resonator array ($a = 5\,\text{mm}, L = 10\,\text{mm}, V = 30 \times 30 \times 30\,\text{mm}^3, b = 40\,\text{mm}$, total number of hole $= 25 \times 25$) [40]

3.1 Finite Element Method (FEM)

In COMSOL Multi-physics software, acoustic pressure in the field of frequency has been employed to model sound absorption which specifies the acoustical behavior of the structure. In this regard, 3D structure is modeled in all simulations. For example, the form of six resonators based on Fibonacci sequence designed in COMSOL Multi-physics has been shown in Fig. (5). In fact, six cavities have been located as neighbor of each other that each cavity is correspond to a specific resonance frequency. In other words, it is possible to increase absorption band by employing 6 cavities with different resonance frequency.

Figs. (6) and (7) show different views of a Helmholtz resonator sample that has been designed in the mentioned software, and how to mesh it, respectively.

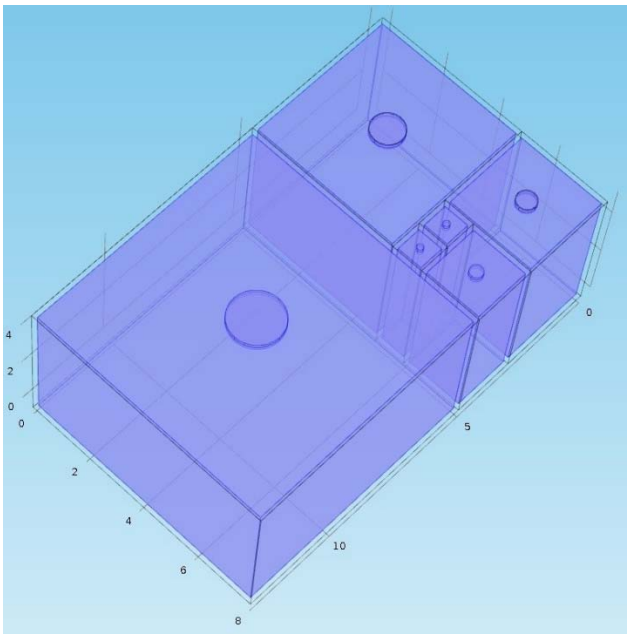

Figure 5 Helmholtz resonator designed in COMSOL Multiphysics software based on Fibonacci sequence

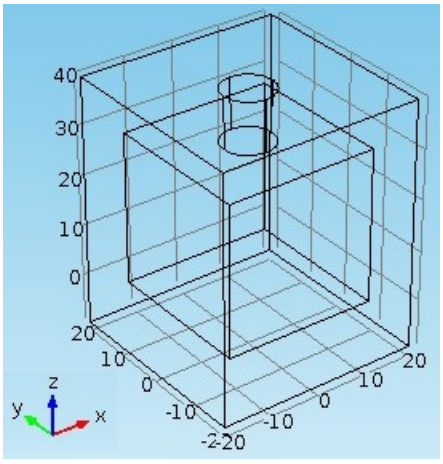

Figure 6 Helmholtz resonator designed in COMSOL Multiphysics software

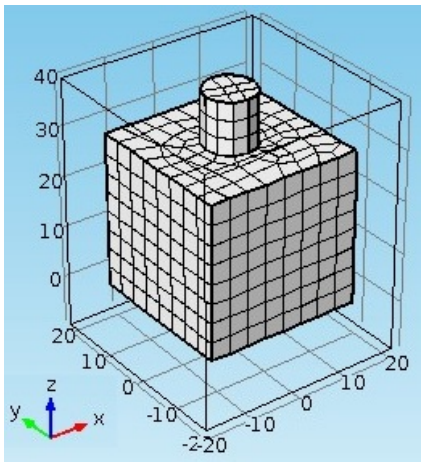

Figure 7 Final cavity mesh of the Helmholtz resonator in COMSOL Multiphysics software

Considering the 3D structure of samples in this paper, both types of mesh elements: swept and free tetrahedral are used in FEM. Also, according to the specifications of the computer, the size of mesh elements are selected finer and extra finer with average number of 181859 elements.

3.2 Boundary condition

As shown in Fig. (8), Helmholtz resonator panel is considered in the free filed. To full fill this condition, the resonators located in the cubic room. The room with free filed condition and the boundary conditions of the room surfaces (wall) are considered "sound full absorptive boundary". Also, it is shown in Fig. (8) that the boundary condition between opening month of resonator block and room is defined by employing Z_R (specific acoustical impedance of the resonator opening based on the section 2.3).

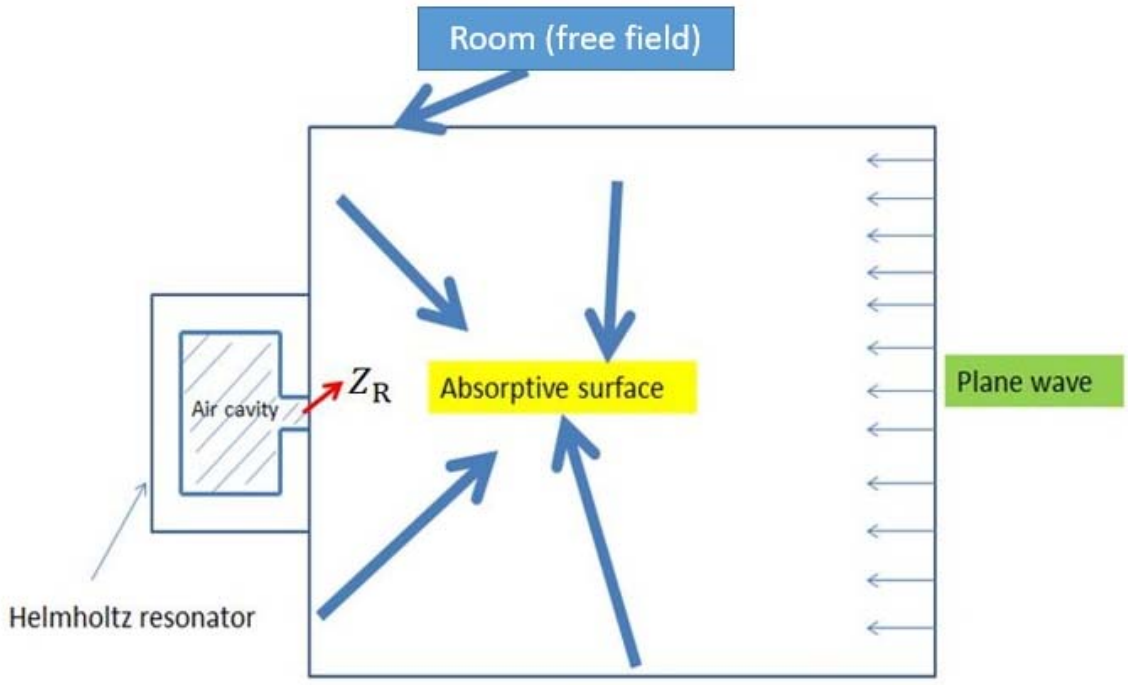

Figure 8 A schematic of the resonator and room wall specification

3.3 sound absorption calculation by FEM

To calculate the sound absorption coefficient of all models, the created models are simulated inside the room in which the walls are fully absorptive.in this regards, by employing the following equation, the pressure reflection coefficient, R, can be calculated.

$$R = \frac{P_r}{P_i} \tag{16}$$

Where, P_r and P_i are the pressure amplitude of the reflected and the incident waves, respectively. Also, the sound absorption coefficient can be calculated by using:

$$\alpha = \frac{Absorbed\ energy}{Incident\ energy} = 1 - |R|^2 \tag{17}$$

In practical, five points in the model are selected near the surface and far from surface of the resonator as shown in Fig. (9) and the average pressure ratio are determined by using the following:

$$\overline{\mathrm{R}} = \frac{1}{5}\sum_{\mathrm{k=1}}^{5} \mathrm{R_n} = \frac{1}{5}\left(\frac{\mathrm{P_{r1}}}{\mathrm{P_{i1}}} + \frac{\mathrm{P_{r2}}}{\mathrm{P_{i2}}} + \frac{\mathrm{P_{r3}}}{\mathrm{P_{i3}}} + \frac{\mathrm{P_{r4}}}{\mathrm{P_{i4}}} + \frac{\mathrm{P_{r5}}}{\mathrm{P_{i5}}}\right) \tag{18}$$

Also, the sound pressure level distribution can be seen in Fig. (10). As shown in the Fig. (10). The amount of the sound pressure of all five points will be chosen from the pressure domain of the room where resonator modeled in.

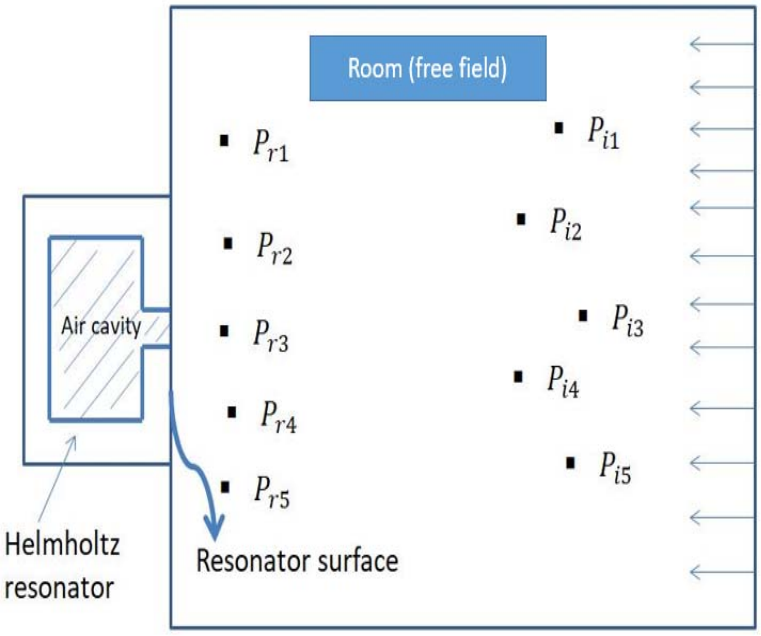

Figure 9 A schematic of the measurement points for incident pressure wave, P_i, and reflected pressure wave, P_r

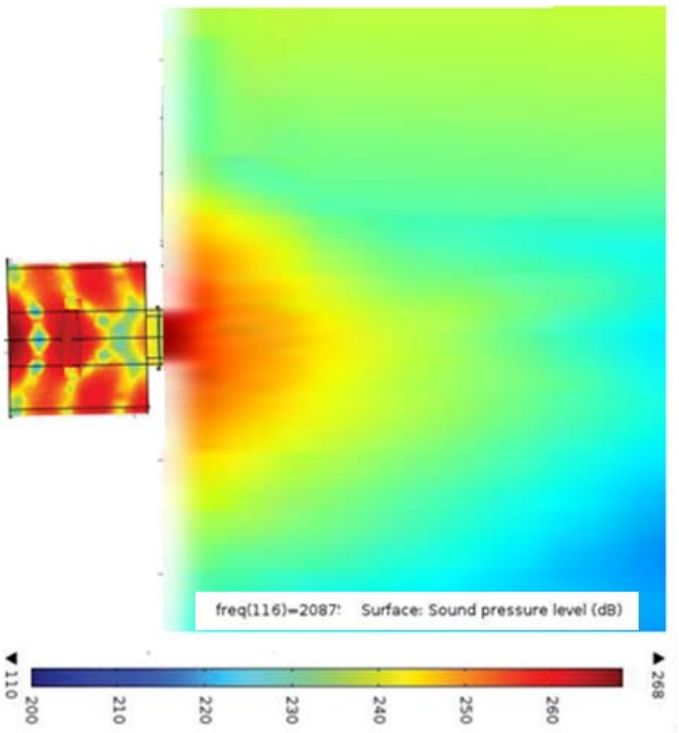

Figure 10 A schematic of the sound pressure level distribution in room and resonator for a model of Helmholtz resonator in COMSOL Multiphysics software

4 Results and Discussions

In this section, Fibonacci based arrangement of different numbers of resonators will be investigated through FEM in COMSOL Multi-physics software (version 5.2) and compared with the results obtained for simulation of periodic array of equal size resonators with the same overall dimensions of block. It means that for a better comparison, the total volume of sound absorber block designed via Fibonacci based resonators arrangement is the same as the total volume of equal size resonators array, in all cases.

4.1 Verification of the FE model with other experimental results

In this section, to validate the simulations performed in the COMSOL Multi-physics software (version 5.2) the results have been compared with those experimentally obtained [40] for two cases: (1) one unit resonator, and (2) four resonators array block with equal size. In this regards, one resonator unit and four resonators array block with equal size are considered with hole diameter, $a = 5\,\text{mm}$, neck length, $L = 10\,\text{mm}$, volume, $V = 27000\,\text{mm}^3$, cross section area $S_b = 10000\,\text{mm}^2$ and $S_b = 2500\,\text{mm}^2$, respectively. As shown in Figs. (11) and (12), the FEM results present good agreement with the experimental results.

The minor differences observed between FEM and experimental results [40] in Figs. (11) and (12) can be attributed to the effects of real boundary conditions in empirical tests. Comparison of Figs. (11) and (12) shows that the sound absorption coefficient of a unit resonator is more than the four resonators array block with equal size. As expected, with the increase in the number of identical resonators in constant volume, the block's overall hardness increases and, as a result, the sound absorption coefficient of the resonator array block decreases.

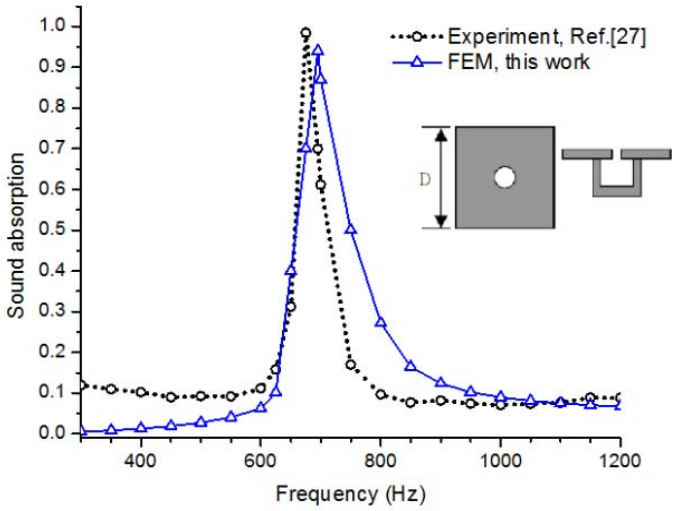

Figure 11 Comparison of the sound absorption coefficient obtained from FEM results and experimental results [40] for one resonator

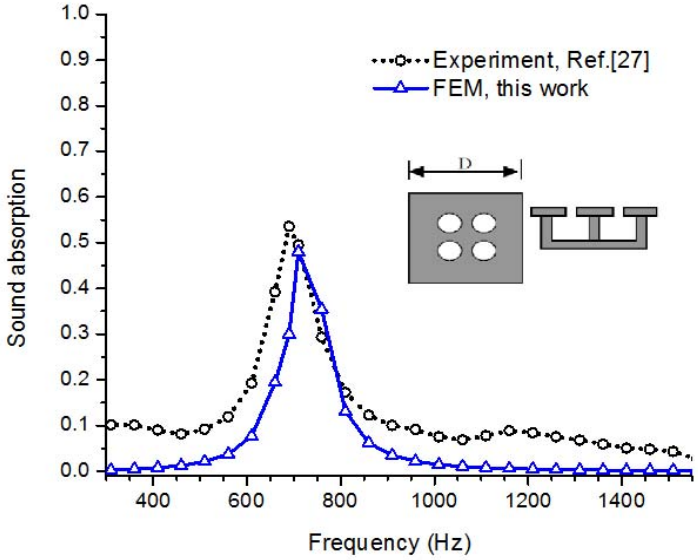

Figure 12 Comparison of the sound absorption coefficient obtained from FEM results and experimental results [40] for four resonators array block with equal size

4.2 Fibonacci model for arrangement of 4 resonators in a sound absorber block

As shown in previous section, the FE model works well. Now, the proposed model employed to design the arrangement of resonators based on Fibonacci sequence. In this regards, the geometry of Fibonacci based-HRA for 4 resonators are as follows:

First resonator: $a = 0.3\,\text{cm}, L = 1\,\text{cm}, V = 3\times3\times5\times10^{-6}\ \text{m}^3, \text{S}_\text{b} = 3\times3\times10^{-4}\ \text{m}^2$

Second resonator: $a = 0.3\,\text{cm}, L = 1\,\text{cm}, V = 3\times3\times5\times10^{-6}\ \text{m}^3, \text{S}_\text{b} = 3\times3\times10^{-4}\ \text{m}^2$

Third resonator: $a = 0.6\,\text{cm}, L = 1\,\text{cm}, V = 6\times6\times5\times10^{-6}\ \text{m}^3, \text{S}_\text{b} = 6\times6\times10^{-4}\ \text{m}^2$

Forth resonator: $a = 0.9\,\text{cm}, L = 1\,\text{cm}, V = 9\times9\times5\times10^{-6}\ \text{m}^3, \text{S}_\text{b} = 9\times9\times10^{-4}\ \text{m}^2$

Fig. (13) shows the sound absorption coefficient versus frequency obtained from FEM for 4 resonators array block (one equivalent resonator with 4 holes) with equal size in comparison with 4 resonators array block based on Fibonacci sequence.

As mentioned before, overall dimensions of 4 resonators array block with equal size have been considered the same as overall dimensions of Fibonacci based resonators array block, $15\times9\times5\times10^{-6}\ \mathrm{m}^3$. Also, the geometrical characteristics of each resonator in periodic same resonator array is considered as :

$a=0.75\ \mathrm{cm}, L=1\ \mathrm{cm}, V=7.5\times4.5\times5\times10^{-6}\ \mathrm{m}^3, \mathrm{S_b}=7.5\times4.5\times10^{-4}\ \mathrm{m}^2$. Fig. (13) illustrates that bandwidth of sound absorption increased by using Fibonacci sequence to array the resonators in a sound absorber block. The reason could be because of increasing the number of Helmholtz resonators with different sizes in Fibonacci based sound absorber block. Since, each resonator has its resonance frequency according to its geometrical characteristics, the overall sound absorption bandwidth of block increases.

Also, average sound absorption increased when Fibonacci based absorber block is employed. This might be due to the overall reduction of the block's stiffness as compared with the case of that the block contains the same number of resonators with the equal sizes. As a result, the block like a spring with less stiffness, vibrates more easily and damps more sound energy.

The same comparison has been carried out for 6 resonators (one equivalent resonator with 6 holes) arrangement in a sound absorber block. The result of this comparison is shown in Fig. (14). For this case, the geometry of Fibonacci resonators set as below:

Note that the sizes of cavities for the resonators 1 to 4 are the same as 4 resonators.

Fifth resonator: $a=1.5\ \mathrm{cm}, L=1\ \mathrm{cm}, V=15\times15\times5\times10^{-6}\ \mathrm{m}^3, \mathrm{S_b}=15\times15\times10^{-4}\ \mathrm{m}^2$

Sixth resonator: $a=2.4\ \mathrm{cm}, L=1\ \mathrm{cm}, V=24\times24\times5\times10^{-6}\ \mathrm{m}^3, \mathrm{S_b}=24\times24\times10^{-4}\ \mathrm{m}^2$

Also, the geometry of each resonator in the 6 resonators array block with equal size is considered as $a=1.3\ \mathrm{cm}, L=1\ \mathrm{cm}, V=13\times12\times5\times10^{-6}\ \mathrm{m}^3, \mathrm{S_b}=13\times12\times10^{-4}\ \mathrm{m}^2$ then, the overall dimensions of sound absorber block designed via Fibonacci based resonators is the same as the overall dimensions of equal size resonators array in sound absorber block, $39\times24\times5\times10^{-6}\ \mathrm{m}^3$.

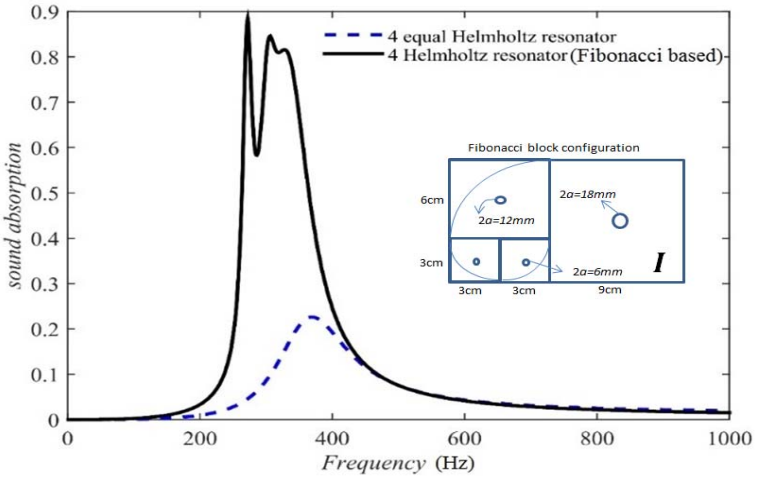

Figure 13 Sound absorption coefficient obtained from FEM results for 4 resonators with equal size in comparison with 4 resonators based on Fibonacci sequence (the size of part *I* are illustrated in fig.12)

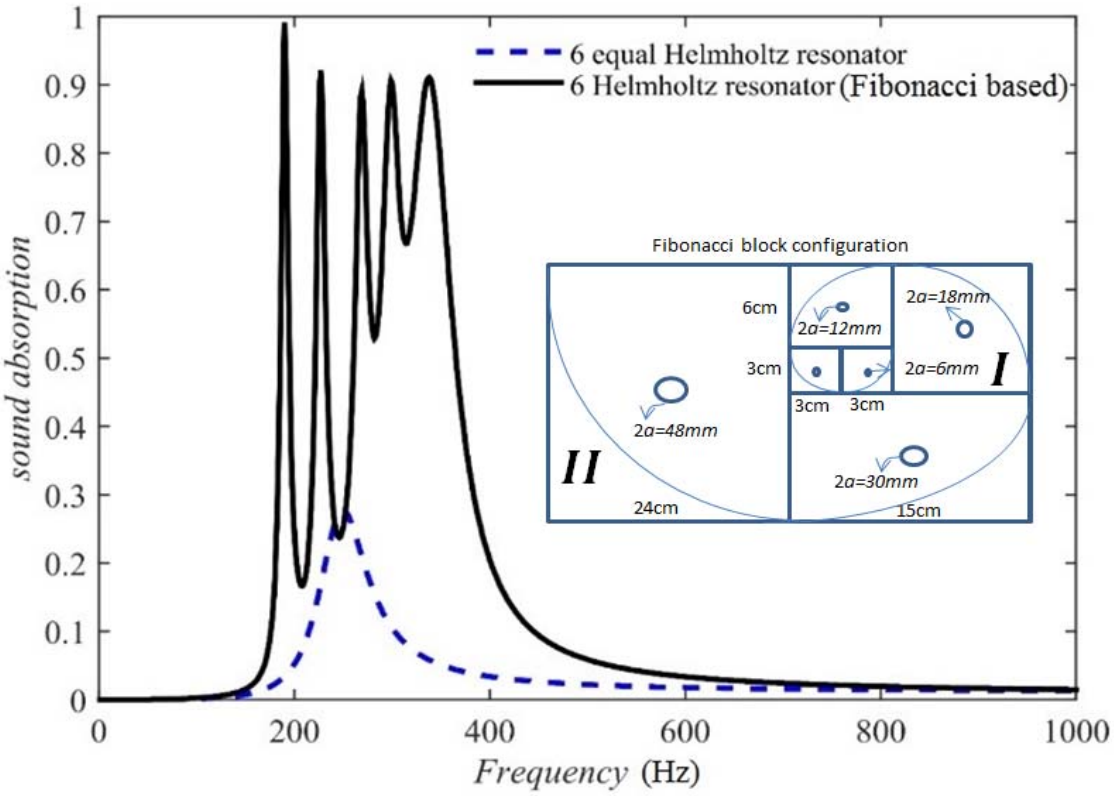

Figure 14 Sound absorption coefficient obtained from FEM results for 6 resonators with equal size in comparison with 6 resonators based on Fibonacci sequence (the sizes of part *I and II* are illustrated in figs.12 and 13, respectively)

4.3 Fibonacci model for arrangement of 6 resonators in a sound absorber block

Fig. (14) illustrates that the bandwidth of sound absorption increased by using Fibonacci sequence in the sound absorber. Also, the average sound absorption increased when Fibonacci absorber is employed. The scientific reason of this case is the same as what explained for Fig. (13). Comparison of Figs. (13) and (14) shows that the sound absorption curve shifts to lower frequencies by using more resonators based on Fibonacci sequence in array absorber block, also sound absorption bandwidth increases without decreasing in amount of sound absorption.

4.4 Fibonacci model for arrangement of 8 resonators in a sound absorber block

In this case, the geometry of Fibonacci resonators are as follows:
The dimensions of the resonators 1 to 6 are the same as the 6 resonators.
Seventh resonator: $a = 3.9\ \text{cm}, L = 1\,\text{cm}, V = 39\times39\times5\times10^{-6}\ \text{m}^3, S_b = 39\times39\times10^{-4}\ \text{m}^2$
Eighth resonator: $a = 6.3\ \text{cm}, L = 1\,\text{cm}, V = 63\times63\times5\times10^{-6}\ \text{m}^3, S_b = 63\times63\times10^{-4}\ \text{m}^2$

The geometry of each resonators in the 8 resonators array block with equal size is considered as $a = 3.15\,\text{cm}, L = 1\,\text{cm}, V = 31.5\times25.5\times5\times10^{-6}\ \text{m}^3, S_b = 31.5\times25.5\times10^{-4}\ \text{m}^2$ so that its overall dimensions is the same as the overall dimensions of sound absorber block designed via Fibonacci based resonators, $102\times63\times5\times10^{-6}\ \text{m}^3$. Fig. (15) shows the sound absorption coefficient versus frequency obtained from FE model results for 8 resonators array block (one equivalent resonator with 8 holes) with equal size in comparison with 8 resonators array block based on Fibonacci sequence.

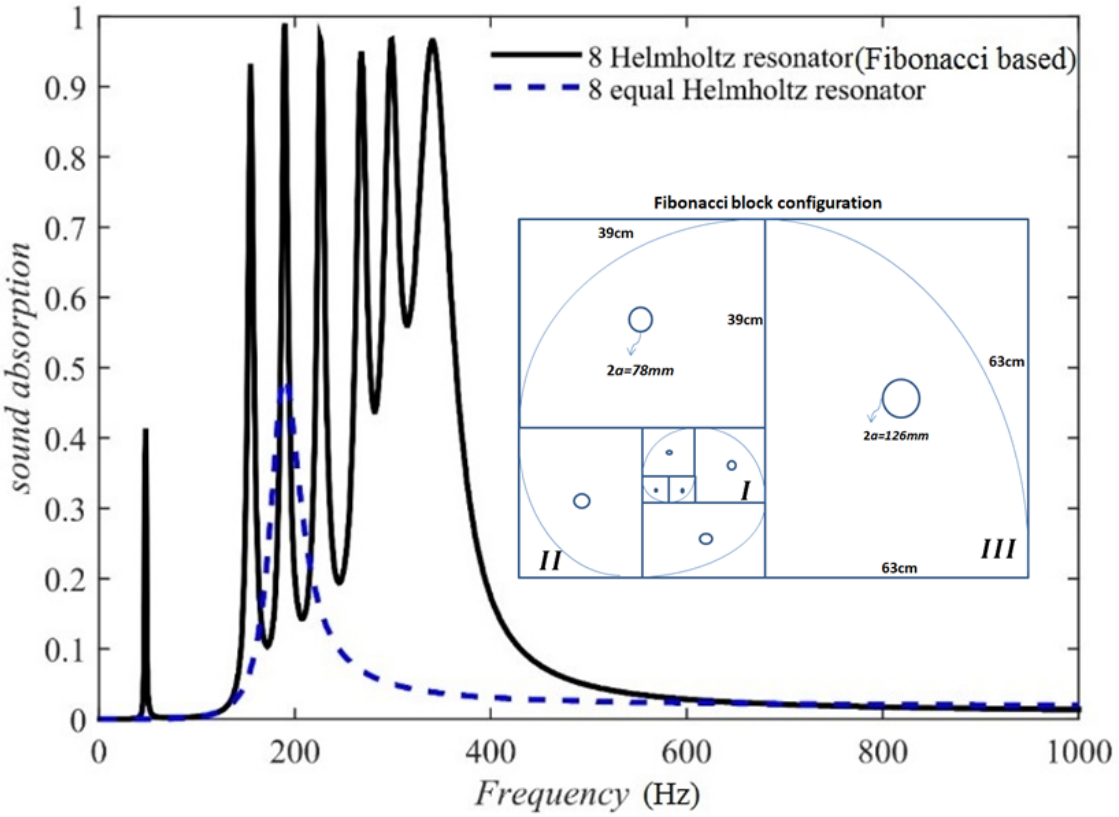

Figure 15 Sound absorption coefficient obtained from FEM results for 8 resonators with equal size in comparison with 8 resonators based on Fibonacci sequence (the sizes of part *I, II and III* are illustrated in Figs.12, 13 and 14, respectively)

As it is shown in Fig. (15), the bandwidth of sound absorption increased by using Fibonacci sequence to design a resonator array block. Also, the average sound absorption increased when Fibonacci sequence is employed to arrange of resonators in a sound absorber block.

4.5 Fibonacci model for arrangement of 10 resonators in a sound absorber block

In the final case study, the geometry of Fibonacci resonators set as below:

The sizes of the resonators 1 to 8 are the same as the 8 resonators.

Ninth resonator: $a=10.2\ \text{cm}, L=1\,\text{cm}, V=102\times102\times5\times10^{-6}\ \text{m}^3, \text{S}_\text{b}=102\times102\times10^{-4}\ \text{m}^2$

Tenth resonator: $a=16.5\ \text{cm}, L=1\,\text{cm}, V=165\times165\times5\times10^{-6}\ \text{m}^3, \text{S}_\text{b}=165\times165\times10^{-4}\ \text{m}^2$

The geometry of each resonators in the 10 resonators array block with equal size is considered as $a=8.25\,\text{cm}, L=1\,\text{cm}, V=82.5\times53.5\times5\times10^{-6}\ \text{m}^3, \text{S}_\text{b}=82.5\times53.5\times10^{-4}\ \text{m}^2$ so that its overall dimensions is the same as the overall dimensions of sound absorber block based on Fibonacci sequence, $267\times165\times5\times10^{-6}\ \text{m}^3$, for a better comparison.

Fig. (16) shows the results of this comparison for sound absorption coefficient of each block versus frequency obtained via FEM.

Fig. (16) demonstrates that the bandwidth of sound absorption increased in Fibonacci based resonators array block. Also, its average sound absorption increased in comparison with equal size resonators array block.

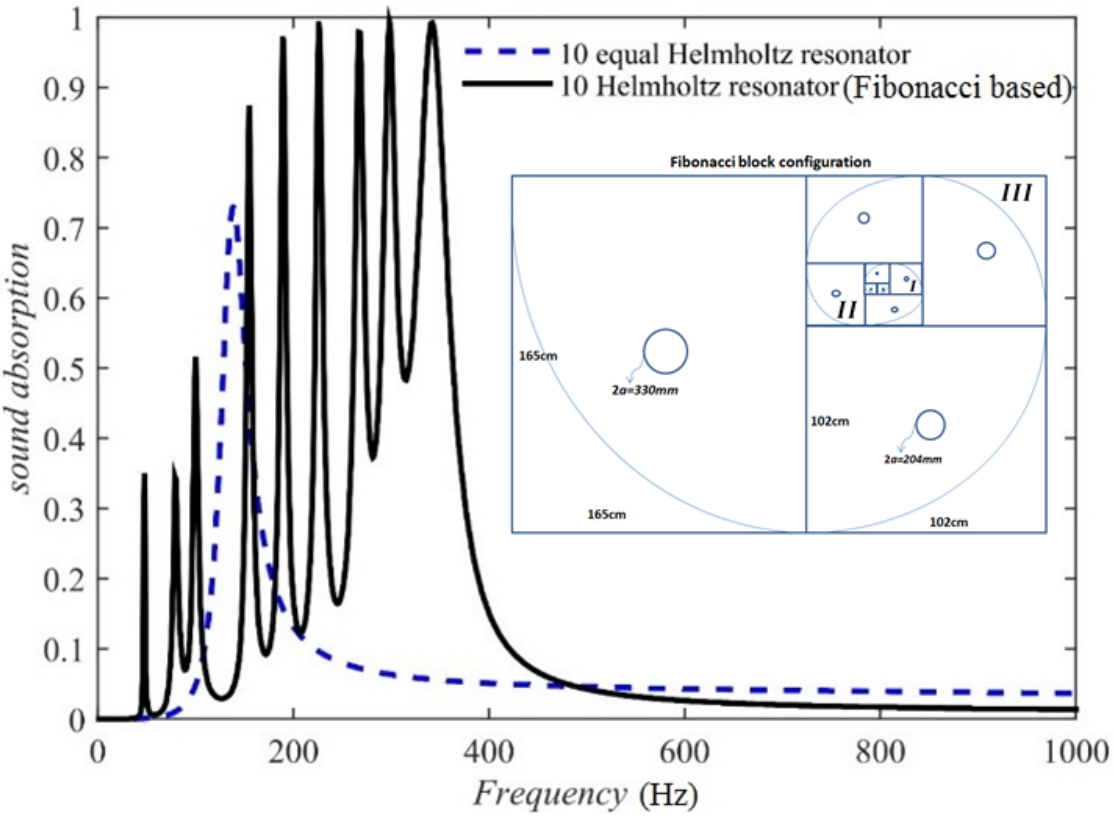

Figure 16 Sound absorption coefficient obtained from FEM results for 10 resonators with equal size in comparison with 10 resonators based on Fibonacci sequence.

5 Conclusions

First, to examine the validity of the results obtained through FEM in COMSOL Multi-physics software, its results compared with the experimental results which obtained by Kim and his colleagues [40] for two cases: (1) a unit resonator, and (2) four resonators array block with equal size. The comparison showed that the FEM presents a good agreement with the results which obtained experimentally [40]. Secondly, to examine the sound absorption performance of Fibonacci based arrangement of different numbers of resonators investigated and compared with the results obtained for the periodic array of equal size resonators through FEM.
In all cases, for a better comparison, the total volume of sound absorber block designed via Fibonacci based resonators arrangement is the same as the total volume of equal size resonators array. The other conclusions can be sort as following:

- The number of frequency resonances increases by using Fibonacci sequence in cross section area and hole diameter of resonant elements in array absorber block.
- Sound absorption bandwidth increases by using Fibonacci sequence to arrange the Helmholtz resonators without decreasing on the magnitude of sound absorption in comparison with equal size resonators array.
- Sound absorption curve shifts to the lower frequencies by using more resonators based on Fibonacci sequence in array absorber block.
- Sound absorption bandwidth increases by using more resonators in Fibonacci based array absorber block without decreasing in amount of sound absorption.

References

[1] Park, J.H., Minn, K.S., Lee, H.R., Yang, S.H., Yu, Ch.B., Pak, S.Y., Oh, Ch.S., Song, Y.S., Kang, Y.J., and Youn, J.R., "Cell Openness Manipulation of Low Density Polyurethane Foam for Efficient Sound Absorption", J. Sound Vib. Vol. 406, pp. 224-236, (2017).

[2] Gwon, J.G., Kim, S.K., and Kim, J.H., "Development of Cell Morphologies in Manufacturing Flexible Polyurethane Urea Foams as Sound Absorption Materials", J. Porous Mater, Vol. 23, pp. 465-473, (2016).

[3] Basirjafari, S., Malekfar, R., and Khadem, S.E., "Low Loading of Carbon Nanotubes to Enhance Acoustical Properties of Poly(ether)Urethane Foams", J. Appl. Phys. Vol. 112, pp. 104312-1 8, (2012).

[4] Kim, B.S., and Park, J., "Double Resonant Porous Structure Backed by Air Cavity for Low Frequency Sound Absorption Improvement", Compos. Struct, Vol. 1, pp. 6-27, (2017).

[5] Zhao, X.D., and Fan, X.Q., "Enhancing Low Frequency Sound Absorption of Microperforated Panel Absorbers by using Mechanical Impedance Plates", Appl. Acoust, Vol. 88, pp. 123-138, (2015).

[6] Selamet, A., and Lee, I., "Helmholtz Resonator with Extended Neck", J. Acoust. Soc. Am. Vol. 113, pp. 1975-1985, (2003).

[7] Sakagami, K., Nagayama, Y., Morimoto, M., and Yairi, M., "Pilot Study on Wideband Sound Absorber Obtained by Combination of Two Different Microperforated (MPP) Absorbers", Acoustic. Sci. Tech. Vol. 30, pp. 154-156, (2009).

[8] Broghany, M., Basirjafari, S., and Saffar, S., "Optimization of Flat Multi-layer Sound Absorber by using Multi-objective Genetic Algorithm for Application in Anechoic Chamber", Modares Mech. Eng. Vol. 16, No. 2, pp. 215-222, (2016).

[9] Broghany, M., Saffar, S., and Basirjafari, S., "Increasing of the Frequency Band of Sound Absorption for Flat Multi-layered Absorbers Consist of Porous Material, Perforated Panel and Air-gap", Amirkabir Journal of Mechanical Engineering, Vol. 50, pp. 219-230, (2018).

[10] Zou, J., Shen, Y., Yang, J., and Qiu, X., "A Note on the Prediction Method of Reverberation Absorption Coefficient of Double Layer Micro-perforated Membrane", Appl. Acoust. Vol. 67, pp. 106-111, (2006).

[11] Ruiz, H., Cobo, P., and Jacobsen, F., "Optimization of Multiple-layer Microperforated Panels by Simulated Annealing", Appl. Acoust. Vol. 72, pp. 772-776, (2011).

[12] Falsafi, I., and Ohadi, A., "Design Guide of Single Layer Micro Perforated Panel Absorber with Uniform Air Gap", Appl. Acoust. Vol. 126, pp. 48-57, (2017).

[13] Yairi, M., Sakagami, K., Morimoto, M., and Minemura, A., "Acoustical Properties of Microperforated Panel Absorbers with Various Configurations of the Back Cavity", Acoust. Sci. & Tech., Vol. 26, pp. 100-110, (2005).

[14] Toyoda, M., and Takahashi, D., "Sound Transmission through a Microperforated-panel Structure with Subdivided Air Cavities", J. Acoust. Soc. Am. Vol. 124, pp. 3594-3603, (2008).

[15] Liu, J., and Herrin, D.W., "Enhancing Micro-perforated Panel Attenuation by Partitioning the Adjoining Cavity", App. Acoust. Vol. 71, pp. 120-127, (2010).

[16] Huang, S., Li, Sh., Wang, X., and Mao, D., "Micro-perforated Absorbers with Incompletely Partitioned Cavities", Appl. Acoust. Vol. 126, pp. 114-119, (2017).

[17] Lu, Y.D., Tang, H., Wang, Q., Tian, J., Qu, Y., and Qiu, B., "The Perforated Panel Resonator with Flexible Tube Bundles and its Applications", J. Acoust. Soc. Am. Vol. 123, pp. 2983-2999, (2008).

[18] Zhang, Q., Lu, Y.D., Yang, J., Wei, X.W., and Wang Y.Q., "Experiment Study on the Sound Absorption Characteristic of Perforated Panel with Ladder Tube Bundles", Noise Vib. Control. Vol. 2, pp. 253-256, (2009).

[19] Li, D., Chang, D., and Liu, B., "Enhancing the Low Frequency Sound Absorption of a Perforated Panel by Parallel-arranged Extended Tubes", Appl. Acoust. Vol. 102, pp. 126-132, (2016).

[20] Wang, Ch., and Huang, L., "On the Acoustic Properties of Parallel Arrangement of Multiple Micro-perforated Panel Absorbers with Different Cavity Depths", J. Acoust. Soc. Am. Vol. 130, pp. 208-218, (2011).

[21] Wang, C.Q., Huang, L.X., and Zhang, Y.M., "Oblique Incidence Sound Absorption of Parallel Arrangement of Multiple Micro-perforated Panels in a Periodic Pattern", J. Sound Vib. Vol. 333, pp. 6828-6842, (2014).

[22] Guo, W., and Min, H., "A Compound Micro-perforated Panel Sound Absorber with Partitioned Cavities of Different Depths", Energy Procedia, Vol. 78, pp. 1617-1622, (2015).

[23] Tang, Y., Ren, Sh., Meng, H., Xin, F., Huang, L., Chen, T., Zhang, Ch., and Lu, T.J., "Hybrid Acoustic Metamaterial as Super Absorber for Broadband Low-frequency Sound", Sci. Rep. Vol. 7, 43340-1 11, (2017).

[24] Li, D., and Cheng, L., "Acoustically Coupled Model of an Enclosure and a Helmholtz Resonator Array", J. Sound Vib. Vol. 305, pp. 272-288, (2007).

[25] Park, S.H., "Acoustic Properties of Micro-perforated Panel Absorbers Backed by Helmholtz Resonators for the Improvement of Low-frequency Sound Absorption", J. Sound Vib. Vol. 332, pp. 4895-4811, (2013).

[26] Seo, S.H., and Kim, Y.H., "Silencer Design by using Array Resonators for Low-frequency Band Noise Reduction", J. Acoust. Soc. Am. Vol. 118, pp. 2332-2338, (2005).

[27] http://www.mcs.zinn-x.com/images/fibonacci-nature-nautilus4.jpg.

[28] http://maths.survey.ac.uk/hosted-sites/R.Knott/Fibonacci Numbers in Real LSife (date of access 24.01.2017).

[29] http://pass.maths.org.uk/issue3/fiibonacci

[30] http://www.mcs.surrey.ac.uk/Personal/R.Knott/Fibonacci/fib.html

[31] http://evolutionoftruth.com/goldensection/goldsect.htm

[32] Hogat, V.E., "Fibonacci and Lucas Numbers", Palo Alto, C: Houghton-Mifflin, (1969).

[33] Horadam, A.F., "A Generalized Fibonacci Sequence", Math Mag, Vol. 68, pp. 455-459, (1961),

[34] Shanon, A.G., and Horadam, A.F., "Generalized Fibonacci Triples", Amer Math Monthly, Vol. 80, pp. 187-190, (1973).

[35] Spinadel, V.W., "The Family of Metallic Means", Vis Math, Vol. 1, pp. 4-8, (1999).

[36] Br´od, D., Piejko, K., and Wloch, I., "Distance Fibonacci Numbers, Distance Lucas Numbers and their Applications", Ars Combinatoria, CXII, pp. 397-410, (2013).

[37] Falcon, S., and Plaza, A., "On the Fibonacci k–numbers", Solitons & Fractals, Vol. 32, pp. 1615-1624, (2007).

[38] Falcon, S., and Plaza, A., "The *k*–Fibonacci Sequence and the Pascal 2–triangle", Chaos, Solit. & Fract, Vol. 33, pp. 38-49, (2007).

[39] Beranek L. L., and VeI. L. r., "*Noise and Vibration Control Engineering-principles and Applications*", Noise and Vibration Control Engineering-Principles and Applications, John Wiley & Sons, Inc.,Vol. 1, pp. 814-819, (1992).

[40] Kim, S.R., Kim, M.S., Kim, Y.H., and Kim, Y.W., "Absorptive Characteristics of Resonator Panel for Low Frequency Noise Control,and its Applications", The 32nd International Congress and Exposition on Noise Control Engineering, Jeju International Convention Center, Seogwipo, Korea, pp. 100-110, August 25-28, (2003),

Nomenclature

α	absorption coefficient
$\vartheta\left(\frac{m^2}{s}\right)$	kinematic viscosity
R	reflection factor
$f(Hz)$	resonance frequency
$\rho\left(\frac{kg}{m^3}\right)$	density
$\omega\left(\frac{1}{s}\right)$	angular frequency
$c\left(\frac{m}{s}\right)$	speed of sound
$z_R\left(\frac{N\cdot s}{m}\right)$	specific acoustical impedance of the resonator
$A(m^2)$	absorption cross section
$Z\left(\frac{N\cdot s}{m^5}\right)$	acoustic Impedance
$z_0\left(\frac{N\cdot s}{m^3}\right)$	characteristic impedance
W_m	sound power
$z_v\left(\frac{N\cdot s}{m}\right)$	volume impedance